OPTOELECTRONIC TWEEZERS – A NEW PARALLEL OPTICAL MANIPULATION TOOL

M.C. Wu[1], A. Jamshidi[1], S.L. Neale[1], M.-C. Tien[1], A.T. Ohta[1,2], and K. Yu[1]
[1]Berkeley Sensor and Actuator Center (BSAC) and Department of Electrical Engineering,
University of California, Berkeley, California, USA
[2]Current address: Department of Electrical Engineering, University of Hawai'i at Manoa

ABSTRACT

Optoelectronic tweezers (OET) [1] has recently emerged as a novel and powerful technique for optical manipulation of microscopic and nanoscopic particles. Previously, OET manipulation and separation of various cell types, polystyrene beads [1,2], and semiconducting and metallic nanowires [3] have been demonstrated.

In this paper, we present some of the recent advances in the optoelectronic tweezers technology. In particular, trapping and manipulation of metallic spherical nanoparticles with diameters below 100 nm [4], parallel assembly of nanowires using lateral-field optoelectronic tweezers (LOET) [5], and assembly of InGaAs/InGaAsP multi-quantum well (MQW) microdisk lasers (201nm thick, 6μm in diameter) using LOET [6,7] are discussed.

KEYWORDS

Optoelectronic Tweezers, Lateral-field Optoelectronic Tweezers, Optical manipulation, Light-induced Dielectrophoresis, Nanowire Assembly, Silicon Photonics, Microdisk Laser Assembly

INTRODUCTION

Several techniques have been developed for manipulation, assembly, and interaction with micro- and nanoscale objects. Among these methods, two main optical manipulation techniques have been used to address this challenge, namely, 1) optical tweezers and 2) optoelectronic tweezers. Optical Tweezers, developed by Ashkin, et al. [8], is a powerful technique for manipulation and study of various particles including cells, polystyrene beads, nanowires, and DNA. In this method, optical gradient forces generated by a highly focused laser source are used to trap particles in solution. One limitation of optical tweezers technique is that stable trapping of particles requires high optical power intensities (~10^7 W/cm^2) which potentially damage the trapped structures and limit the operational working area.

Optoelectronic tweezers (OET) operates based on the principle of *optically-induced* dielectrophoresis (DEP) force. In the conventional electrode-based DEP [9], a non-uniform electric field is created between two lithographically defined electrodes. This field induces a dipole on the particles present in the vicinity of the electrodes and either attracts or repels them from areas of highest field intensity, depending on the relative polarizability of the particles to the medium. A limitation of fixed-electrode DEP manipulation is that the trapping sites are static, therefore, it is incapable of real-time and flexible manipulation of trapped particles. OET overcomes this challenge by defining the electrodes virtually, through the interaction of a light source with a photoconductive material, hydrogenated amorphous silicon (a-Si:H). Moreover, since the light source is not used to directly trap the particles, only to define the virtual electrodes, OET is capable of manipulating particles with 100,000× less optical power intensity than optical tweezers.
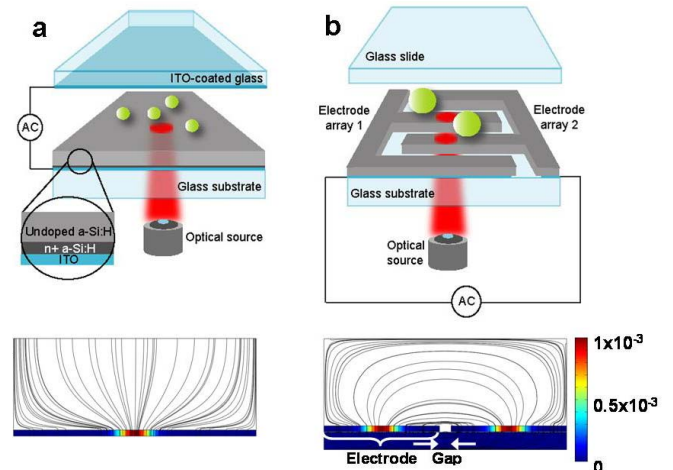

Figure 1: (a) Conventional and (b) Lateral-field OET device structures and simulated electric field lines for each case. Reproduced from [10].

Figure 1a shows the structure of the conventional OET device [10] which consists of a bottom indium-tin-oxide (ITO) electrode on top of which there is 1-2 μm of a-Si:H deposited and a top ITO electrode. The liquid layer containing the particles of interest is sandwiched between the two electrodes and there is an AC bias applied between the two ITO electrodes. When a-Si:H is exposed to a light source, electron-hole pairs are generated in the a-Si:H layer, increasing its conductivity and transferring the voltage to the liquid layer, only in the area that the light source is present. This creates a non-uniform electric field in the liquid layer, attracting or repelling particles from areas of highest field intensity due to the DEP principle. The DEP force [9] experienced by a spherical particle is:

$$F_{DEP} = 2\pi r^3 \varepsilon_m \, \mathrm{Re}\{K^*(\omega)\}\nabla E^2 \qquad (1)$$

$$K^*(\omega) = \frac{\varepsilon_p^* - \varepsilon_m^*}{\varepsilon_p^* + 2\varepsilon_m^*}, \; \varepsilon_m^* = \varepsilon_m - j\frac{\sigma_m}{\omega}, \; \varepsilon_p^* = \varepsilon_p - j\frac{\sigma_p}{\omega}$$

where r is the radius of the particle, $_m$ and $_p$ are the permittivities of the medium and the particle respectively, $_m$ and $_p$ are the conductivities of the medium and the particle respectively, is the frequency of the AC bias, $Re\{K^*( )\}$ is the real part of the Clausius-Mossotti (C.M.) factor $K^*( )$, and ∇E^2 is the gradient of electric field intensity.

Figure 1b shows the device structure for a variation of the OET device, called lateral-field optoelectronic tweezers (LOET) [10]. In the conventional OET device, the field lines are perpendicular to the bottom and top surfaces. Anisotropic particles such as nanowires align their long-axis with the field lines due to the torque experienced. Therefore, in conventional OET device such particles are manipulated perpendicular to the device surface. However, in many device assembly applications, it is desired to have the wires in parallel to the device surface for better positioning and alignment. LOET overcomes this challenge by patterning the bottom a-Si:H surface in the form of interdigitated electrodes and applying an AC bias between the electrodes. This results in electric field lines in parallel with the manipulation plane and simplifies the assembly process.

In the following sections, we discuss some of the recent advances in micro and nanostructure manipulation and assembly achieved using OET and LOET platforms.

METALLIC NANOPARTICLE MANIPULATION

Metallic nanoparticles have recently received much attention as local and sub-diffraction limited nano-sensors for chemical and biological sensing [11]. However, interaction with such nanoscopic objects has proved to be challenging. Optical tweezers have been used for trapping and confinement of metallic nanoparticles [12]. However, the high required optical intensities ($\sim 10^7$ W/cm^2) result in excessive heating ($\Delta T>55°C$) [13], limiting practical application of trapped particles in biological sensing. DEP force has also been used to trap nanoparticles [14], however, the fixed trapping patterns do not allow for dynamic scanning of the trapped particles.

OET can overcome these challenges by trapping metallic nanoparticles using optical intensities 100,000× smaller than optical tweezers, therefore, significantly reducing the heating in particles due to absorption. Moreover, the optical traps can be dynamically controlled which overcomes the challenge of fixed trapping patterns.

Figure 2 shows trapping and transport of an individual 100 nm diameter gold nanoparticle trapped using OET [4]. The laser source is scanned manually across the stage over $\sim$200 μm^2 area and the nanoparticle follows the trap. Since the DEP force is proportional to the volume of the particle, the magnitude of the force drops rapidly for nanoscale objects. However, in the OET device, the strongest field intensity gradients, ∇E^2, are present near the a-Si:H surface, therefore, the metallic nanoparticles are immersed

in the highest ∇E^2 region due to their small sizes. This overcomes the reduction in DEP force due to particles small radii. We have characterized the maximum translational velocities of 100nm diameter gold nanoparticles to be $\sim$68 $\mu m/s$ at 20Vpp. This corresponds to a DEP force of $\sim$0.1pN.
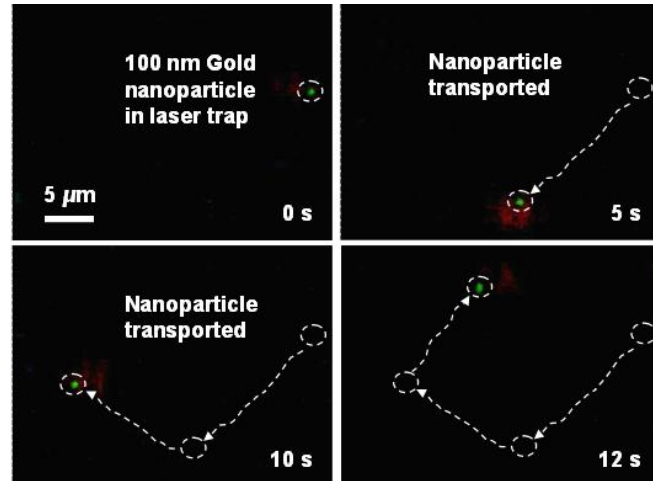

Figure 2: OET trapping and transport of a single 100nm diameter gold nanoparticle. The nanoparticle experiences a positive DEP force and follows the laser trap. The trapped nanoparticle is transported over $\sim$200μm^2 area within 12 seconds. Reproduced from [4].

In addition to trapping of single particles, OET is capable of concentration of multiple nanoparticles in a single trap as shown in figure 3. Five 250nm diameter gold nanoparticle are trapped and transported using OET. This capability is important in enhancing the sensitivity of such dynamic nano-sensors.
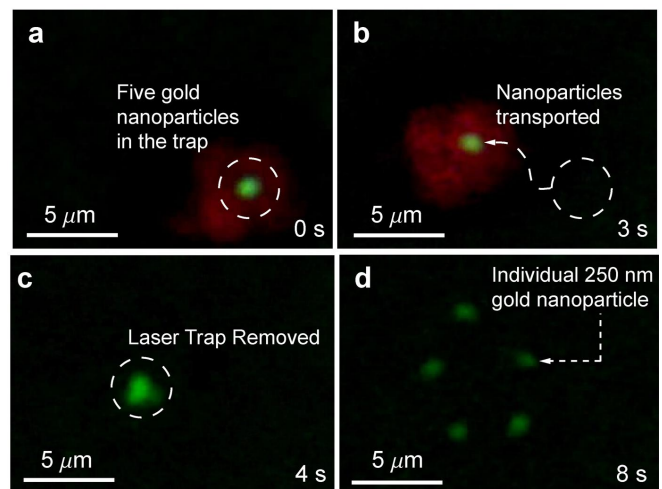

Figure 3: (a-d) Trapping and transport of five 250nm gold nanoparticles. The nanoparticles are concentrated in the laser trap. Once the laser is removed, the particles undergo Brownian motion and are distinctly visible. Reproduced from [4].

1583

PARALLEL ASSEMBLY OF NANOWIRES

Nanowires have been studied extensively in recent years as suitable building blocks for opto- and nanoelectronic devices [15]. In addition, various synthesis and characterization techniques have been developed to create a large array of semiconducting, metallic, and insulating nanowires with various properties. However, the bottom-up integration of nanowires to create large-scale devices still remains challenging. Many techniques such as mechanical manipulation [16], optical tweezers [17], and fixed-electrode DEP [18] have been used for post-synthesis integration of individual nanowires. However, these methods are either limited in throughput or lack flexible manipulation capability.

Conventional OET is capable of large-scale and low optical power manipulation of particles and has been used previously to trap and separate semiconducting and metallic nanowires [3]. However, due to the alignment of nanowires long-axis with the vertical field, the positioning and integration is difficult. Alternatively, LOET is capable of manipulation of nanowires in a lateral fashion which is more suitable for device assembly [5].

Figure 5(a-c) shows the process of fabricating a silver nanowire array using a new variation of LOET device (shown in Figure 4). Silver nanowires of 80-100nm diameter and 1-10μm length dispersed in an ethanol solution were used for the experiments. A 300 mVpp at 200kHz AC bias is applied between the interdigitated metal electrodes and optical patterns are generated using a digital micromirror display (DMD) device. The nanowires are then attracted to the high electric field intensity areas near the tip of the paired triangular light patterns. After the trapping process is complete, the applied AC voltage is increased to 2.8Vpp, attracting the nanowires strongly to the bottom surface and permanently immobilizing them. Subsequent scanning electron microscopy (SEM) image of the assembled nanowires is shown in figure 5d.
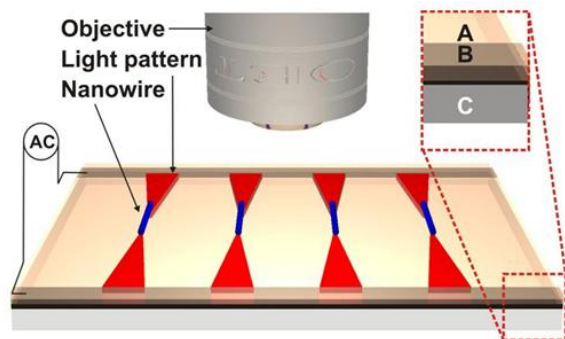

Figure 4: New LOET device structure. Layers A, B, and C indicate: unpatternd a-Si:H, aluminum electrode, and oxidized silicon wafer, respectively. There is an AC bias applied between the metal electrodes which are extended by paired triangular light patterns for in-plane nanowire manipulation and assembly. Reproduced from [5].
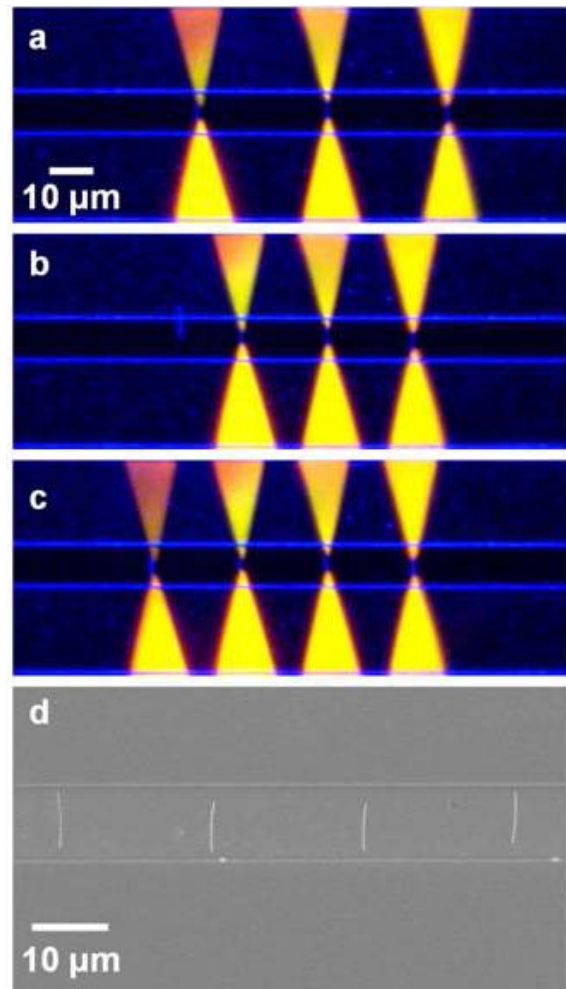

Figure 5: Assembly of four silver nanowires into an array using LOET. (a) Three nanowires are captured in the trap using paired triangular light patterns. (b) The nanowires are moved closer to each other by adjusting the position of light patterns. (c) Another nanowire is captured and added to the array. (d) SEM image of assembled nanowire array. Reproduced from [5].

MICRODISK LASER ASSEMBLY

On chip integration of semiconductor lasers with CMOS circuitry has attracted much interest in recent years. Several techniques have been used to accomplish such integration including Silicon Raman lasers [19], which is limited in that it still requires external laser optical pumping; epitaxial growth of III-V lasers on Silicon substrate [20] which requires too high of a temperature (>400°C) for post-CMOS processing, and low-temperature wafer bonding [21] which is limited due to strict planarity requirements.

LOET assembly of pre-fabricated III-V microdisk lasers on fully processed CMOS wafers offers a novel room-temperature optofluidic solution for CMOS integration [6,7]. Figure 6 shows the LOET device structure for microdisk laser manipulation and the process of assembling an InGaAs/InGaAsP multi-quantum-well

1584

(MQW) microdisk laser (201nm thick and 6μm in diameter). Once the microdisk is assembled the applied AC voltage is increased to hold the assembled microdisk in place during the drying process. Figure 7(a) shows the SEM image of the assembled microdisk.
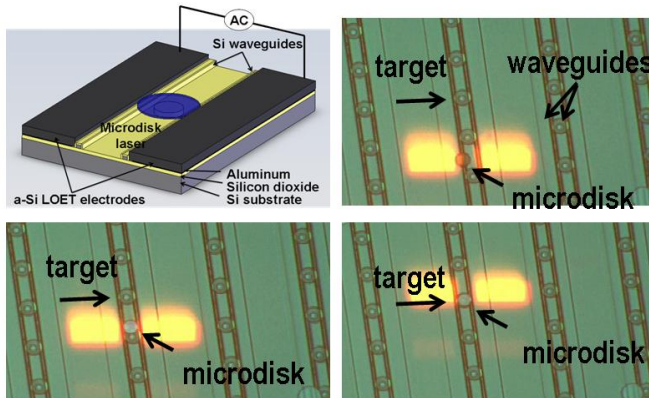

Figure 6: LOET device structure for microdisk laser assembly and the assembly process of an InGaAs/InGaAsP MQW microdisk laser. Reproduced from [7].

Figures 7(b) and 7(c) show the measured laser output versus pump power (L-L curve) and the measured optical spectrum, respectively.
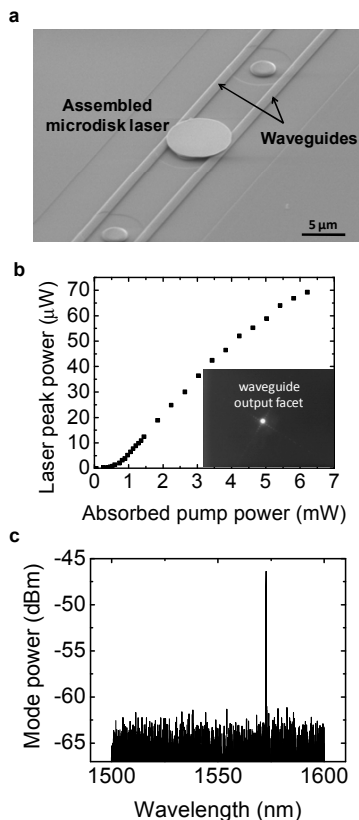

Figure 7: (a) SEM image of an assembled microdisk laser using LOET. (b) measured laser output versus pump laser (L-L) curve. (c) measured optical spectrum. Reproduced from [7].

An effective threshold peak pump power of 0.6mW is measured. The external quantum efficiency of the laser coupling to the waveguide measured at a single end is 3.5%. Using an 8.8mW pump laser, we obtain a maximum laser output power of 90μW. In addition, single mode operation with 1572.6nm peak wavelength is observed.

CONCLUSION

In conclusion, optoelectronic tweezers provides an exciting novel optofluidic platform for manipulation of micro and nanoscale objects. In this paper, we reviewed some of the recent advances in manipulation of various structures using OET. In particular, trapping and manipulation of spherical metallic nanoparticles with diameters below 100 nm, parallel assembly of silver nanowires with 80-100nm diameter and 1-10μm length using LOET, and optofluidic assembly of prefabricated InGaAs/InGaAsP MQW microdisk lasers with 201nm thickness and 6μm length using LOET were discussed.

REFERENCES

[1] P.Y. Chiou, A. T. Ohta, M. C. Wu, *Nature,* vol. 436, pp. 370 372, 2005.
[2] A. T. Ohta, *IEEE Journal of Selected Topics in Quantum Electronics*, vol. 13, 235-243, 2007.
[3] A. Jamshidi, et al., *Nature Photonics*, vol. 2, pp. 85 - 89, 2008.
[4] A. Jamshidi, et al., in IEEE MEMS Conference, 2009.
[5] A. T. Ohta, et al., in IEEE/LEOS International Conference on Optical MEMS and Nanophotonics, 2008, pp. 7-8.
[6] M.-C. Tien, et al., *Appl. Phys. A*, DOI 10.1007/s00339-009 51252, 2009.
[7] M.-C. Tien, et al., in Optical Fiber Communication (OFC) Conference, San Diego, 2009.
[8] A. Ashkin, et al., *Physical Review Letters*, vol. 24, 1970.
[9] T. B. Jones, *Electromechanics of Particles* (Cambridge: Cambridge University Press), 1995.
[10] A. T. Ohta, et al., in CLEO Conference, 2007, pp. 1-2.
[11] J. N. Anker, et al., *Nature Materials*, vol. 7, pp. 442 - 453, 2008.
[12] K. Svoboda and S. M. Block, *Optics Letters*, vol. 19, pp. 930-932, 1994.
[13] Y. Seol, A. E. Carpenter, T. T. Perkins, *Opt. Lett*, vol.. 31, pp.1937 - 1942, 2006.
[14] L. Zheng, L., et al., *Langmuir*, vol. 20, pp.8612-8619, 2004.
[15] Y. Xia, et al., *Advanced Materials*, vol. 15, pp. 354-389 2003.
[16] D. J. Sirbuly, et al., *Proc. Natl Acad. Sci. U. S. A.,* vol. 102, pp. 7800-7805, 2005.
[17] P. J. Pauzauskie, et al., *Nature Materials,* vol. 5, pp. 97-101, 2006.
[18] Seo, H. W., et al., *Nanotechnology,* vol. 17, pp. 3388-3393, 2006.
[19] H. Rong, et al., *Nature*, vol. 433, pp. 725-728, 2005.
[20] G. Balakrishnan, et al., *IEEE J. Select. Topics Quantum Electron.*, vol. 12, pp.1636-1641, 2006.
[21] Van Campenhout, J., et al., *Opt. Express*, vol. 15, pp.6744 6749, 2007.